

A Fast Super-Resolution Method Based on Sparsity Properties

Yuanchao Bai¹, Huizhu Jia^{*1}, Xiaodong Xie¹, Rui Chen¹, Ming Jiang², Wen Gao¹

¹*School of Electronics Engineering and Computer Science, Peking University, Beijing 100871, China*

{yuanchao.bai, hzjia, donxie, chenrui2014, wgao}@pku.edu.cn

²*Department of Information Sciences, School of Mathematical Sciences, Peking University, Beijing 100871, China*

ming-jiang@pku.edu.cn

Abstract—Super-resolution enhancement is a kind of promising approach to enhance the spatial resolution of images. To super-resolve a satisfying result, regularization term design and blur kernel estimation are two important aspects which need to be carefully considered. In this paper, we propose a robust regularized super-resolution reconstruction approach based on two sparsity properties to deal with these two aspects. Firstly, we design a sparse reweighted TV L_1 prior to restrict the first derivative of the upsampled image. Then, noticing that only deblurring sparse high gradient areas can sharpen the super-resolution result, we design an over-deblurring control method to decrease the artifacts caused by inaccurate blur kernel estimation. We also design a fast optimization algorithm to solve our model. The experimental results show that the proposed approach achieves a remarkable performance both in visual quality and run time.

Index Terms—Super-resolution, Regularization construction, Sparsity properties, Over-deblurring control, Convex optimization.

I. INTRODUCTION

As the resolution of consumer electronics is becoming higher and higher, lots of low resolution (LR) images and videos need to be upsampled to display. Besides, many smart phone companies begin to use upsampling algorithms to improve the performance of their phone camera system. Therefore, the research on fast and robust image and video upsampling algorithms has drawn a lot of attentions now.

Super-resolution (SR) (e.g. [1]) is a promising technology for image upsampling, which is usually better than image interpolation. The original image SR algorithms restore a high resolution (HR) image from multiple LR images of the same scene. These LR images are sub-pixel precision warped, so more information can be extracted from LR images to generate a HR image. However, as the sub-precision images are not usually available, researchers are seeking ways to super-resolve a HR image from a single LR image.

Single-image SR can usually be achieved by regularized SR reconstruction approaches or example-based SR approaches. Example-based SR approaches perform well or even better

than regularized SR reconstruction approaches in some occasions, but their drawbacks are obvious. Example-based SR approaches need to train a dictionary, which costs memory to store and can only be used in fixed upsampling factors. Besides, training a dictionary and matching patches in the dictionary are very time-consuming.

Regularized SR reconstruction approaches are free from the drawbacks of example-based SR approaches. Recent researches of this kind (e.g. [2], [3], [4]) are all based on the SR observation model and design different regularization terms to restore HR images. Regularized SR reconstruction approaches usually include two parts: interpolation and deblurring. The main difficulties of regularized SR reconstruction approaches are the regularization term design and blur kernel estimation. Improper regularization term and blur kernel estimation will cause ringing artifact and the noise amplification in restored HR results.

In this paper, we take advantage of two sparsity properties and propose a novel fast and robust regularization SR reconstruction algorithm. The first sparsity is that the distribution of derivative filters in natural image is sparse. Levin et al. [5] proposed an image deblurring approach using TV L_p norm ($0 < p < 1$) as the regularization term and achieved a good result without ringing artifact. However, as the TV L_p norm ($0 < p < 1$) is not convex, they solved their model using conjugate gradient algorithm in spatial domain which was very slow. Different from the TV L_p norm ($0 < p < 1$), we use reweighted TV L_1 norm first proposed by Candes et al. [6] as the sparse prior and design the weights to make the reweighted TV L_1 norm curve similar to TV L_p norm ($0 < p < 1$). We also design a fast optimization algorithm to solve the reweighted TV L_1 norm regularization by using alternating direction method of multipliers (ADMM) and proximal algorithm [7]. The second sparsity is that only the high gradient area needs to be deblurred in the SR process. Over-deblurring in smooth area only amplifies noise and introduces ringing artifact. We design a multi-resolution based method to distinguish high gradient area from low gradient area to make a mask to help control the over-deblurring artifacts.

The rest of this paper is organized as follows. Section II summarizes the related works. Section III describes the proposed algorithm. Section IV discusses the experiment results. Finally, in section V the conclusions are presented.

* The corresponding author.

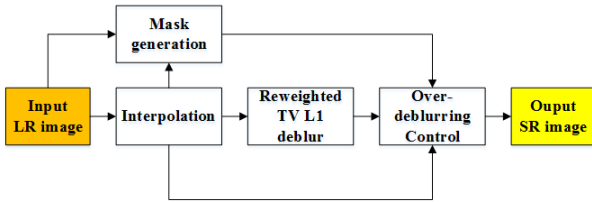


Fig. 1. Diagram of the proposed SR algorithm.

II. RELATED WORKS

In this section, we review the previous works on single-image SR approaches: example-based SR approaches and regularized SR reconstruction approaches.

Example-based SR approaches are based on statistical learning. Noticing that small patches of natural images tend to recur many times in the scales that an observer can or cannot visually perceive, Freeman et al. [8] trained a LR/HR dataset from natural images, matched LR patches to find corresponding HR patches in the dataset and then combined them to achieve HR result. Similarly, Chang et al. [9] trained the dataset and solved the weights of matched LR images by manifold learning method LLE. Yang et al. [10] used sparsity as a prior for dataset training and showed that a small set of randomly chosen raw patches of similar statistical nature can be trained as a good sparse dictionary. Glasner et al. [11] introduced a unified framework for combining multi-image SR and self-example-based SR. Their approach exploited patch-similarity within and across scales to construct HR image.

Regularized SR reconstruction approaches model SR process as an ill-posed reconstruction problem. Shan et al. [2] proposed a gradient distribution prior and a feedback-control framework which faithfully recovered the HR image from input data. Sun et al. [3] proposed an SR approach using gradient profile prior learned from natural images. Shen et al. [4] considered viewers' perceptual blur radius and retinal image size to estimate Gaussian blur level for the SR reconstruction.

III. SUPER-RESOLUTION BASED ON SPARSITY PROPERTIES

In the proposed algorithm, we take advantage of two sparsity properties to upscale the input LR image. We first super-resolve the input LR image using regularized SR reconstruction with reweighted TV L_1 prior. The reweighted TV L_1 prior, which enhances sparsity of the first derivative of the reconstructed SR result, results in a sharp SR output. Considering that deblurring only in sparse high gradient area can help sharpen the interpolated image, we use multi-resolution method to distinguish high gradient area from low gradient area to make a mask to help control the over-deblurring artifacts. Fig. 1 shows the diagram of our algorithm.

A. SR Reconstruction using Reweighted TV L_1 Prior

According to the observation model, single LR image is usually assumed to result from blurring, downsampling and

noise addition, which can be formulated as (1),

$$\mathbf{y} = \mathbf{D} \cdot (\mathbf{B} \otimes \mathbf{x}) + \mathbf{n} \quad (1)$$

where \mathbf{x} is the unknown HR image, \mathbf{B} is the blind blur kernel, \otimes is convolution process and \mathbf{D} is the downsampling process. \mathbf{n} is the image noise, which is usually modeled as a set of independent and identically distributed (i.i.d.) Gaussian noise. \mathbf{y} is the observed LR image. Here we assume that upsampled i.i.d Gaussian noise is still i.i.d Gaussian noise, so the inverse process can be formulated as (2),

$$\mathbf{x} = \mathbf{B} \otimes^{-1} \mathbf{D}^{-1} \cdot \mathbf{y} + \mathbf{n} \quad (2)$$

where \mathbf{D}^{-1} is the interpolation process and \otimes^{-1} is deconvolution.

The difficulty of implementing interpolation and deblurring is that interpolation methods are various and the blur kernel is unknown. We consider interpolation selection and blur kernel estimation together. As 2D Gaussian kernel is the most widely used blur kernel in image processing and can approximately model other blur kernel by adjusting kernel size and the standard deviation, we estimate \mathbf{B} as 2D Gaussian kernel. To select an interpolation, we have tried bilinear, bicubic, NEDI [12]. We find that different interpolation methods do not influence the deblurred result much in our model. For the sake of simplicity, we select bilinear interpolation.

Since we have the interpolated image, we can do the Gaussian deblurring process. As the distribution of derivative filters in natural image is sparse, we incorporate the reweighted TV L_1 norm prior to enhance the sparsity of the first derivative of the deblurred result in our model. The model is formulated as (3),

$$\min_{\mathbf{x}} \frac{1}{2} \sum_{i,j} \|(\mathbf{B} \otimes \mathbf{x} - \mathbf{b})_{i,j}\|_2^2 + \mu \sum_{i,j} \left(w_x^{i,j} \|(\mathbf{V}_x \mathbf{x})_{i,j}\|_1 + w_y^{i,j} \|(\mathbf{V}_y \mathbf{x})_{i,j}\|_1 \right) \quad (3)$$

where \mathbf{b} is the interpolated image, \mathbf{V}_x and \mathbf{V}_y are the horizontal and vertical first derivative filter. μ is the weight coefficient of regularization term. $w_x^{i,j}$ and $w_y^{i,j}$ are the weights for horizontal and vertical derivative in each pixel (i, j) , which are constant when solving (3).

We use (4) to calculate the weights for our prior in each iteration,

$$w_{i,j}^{k+1} = \frac{2}{|(\mathbf{V}\mathbf{x})_{i,j}^k| + 1} \quad (4)$$

where $w_{i,j}^{k+1}$ in pixel (i, j) is calculated by the first derivative in the k -th iteration.

Fig. 2 shows the 1D curve of L_1 norm, $L_{0.8}$ norm [5] and reweighted L_1 norm whose weights are calculated by (4). The curve of our reweighted L_1 norm, which is similar to $L_{0.8}$ norm, is actually sparsity enhanced.

In order to solve (3) with proximal algorithm [7] and ADMM, we reformulate (3) in matrix representation and

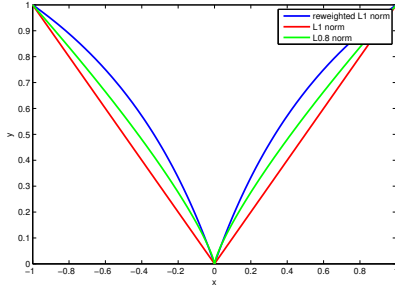


Fig. 2. Function curve of L_1 norm, $L_{0.8}$ norm and reweighted L_1 norm priors.

introduce two auxiliary variables \mathbf{z} and \mathbf{y} , as shown in (5). Unlike optimization problem in [5], (5) is convex.

$$\begin{aligned} \min_{\mathbf{x}, \mathbf{z}, \mathbf{y}} \quad & \frac{1}{2} \|\mathbf{B}\mathbf{x} - \mathbf{b}\|_2^2 + \mu \|\mathbf{W}\mathbf{z}\|_1 + \frac{\rho}{2} \|\mathbf{V}\mathbf{x} - \mathbf{z} + \frac{\mathbf{y}}{\rho}\|_2^2 \\ \text{s.t.} \quad & \mathbf{V} = \begin{bmatrix} \mathbf{V}_x \\ \mathbf{V}_y \end{bmatrix} \end{aligned} \quad (5)$$

\mathbf{W} is diagonal matrix with weights on the diagonal. The optimization algorithm is demonstrated as follows.

Algorithm 1 ADMM for Reweighted TV L_1 norm.

Input:

Set \mathbf{B} , \mathbf{V} , \mathbf{b} , μ , ρ and k_{max} ;

Initialize $k = 0$, $\mathbf{y}^k = \mathbf{0}$, $\mathbf{z}^k = \mathbf{0}$ and $\mathbf{W}^k = \text{diag}(1)$;

Output:

Deblurred Image \mathbf{x} ;

1: Solve the reweighted TV L_1 using ADMM:

while not converge **do**

$$\mathbf{x}^{k+1} = (\mathbf{B}^T \mathbf{B} + \rho \mathbf{V}^T \mathbf{V})^{-1} (\mathbf{B}^T \mathbf{b} - \mathbf{V}^T \mathbf{y}^k + \rho \mathbf{V}^T \mathbf{z}^k),$$

$$z_i^{k+1} = \text{prox}_{\mu w_i \rho^{-1}}((\mathbf{V}\mathbf{x}^{k+1} + \frac{\mathbf{y}^k}{\rho})_i), \quad \text{for all } i$$

$$\mathbf{y}^{k+1} = \mathbf{y}^k + \rho(\mathbf{V}\mathbf{x}^{k+1} - \mathbf{z}^{k+1}).$$

endwhile

2: Update the weights for each element:

$$w_i^{k+1} = \frac{2}{|(\mathbf{V}\mathbf{x})_i^k| + 1}$$

3: Terminate on convergence or when k attains k_{max} . Otherwise, $k = k + 1$ and go to Step 1;

4: **return** \mathbf{x} ;

Because matrix \mathbf{B} and \mathbf{V} are Block Toeplitz, ADMM can rapidly be solved in frequency domain using **fft2**.

B. Over-deblurring Control

Although reweighted L_1 Prior can help decrease the artifact, the ringing artifact and noise amplification can still happen

because the Gaussian blur kernel sometimes cannot match the real blur process and some areas are over-deblurred. In order to control the over-deblurring, we take the advantage of the second sparsity.

We find that deblurring only in the high gradient area can sharpen the interpolated image and usually the area is sparse. On the contrary, deblurring in the smooth area can easily cause artifacts and usually the smooth area is dense. So we decide to distinguish the high gradient area from low gradient area to make a mask, then apply deblurring only in high gradient area to help control the over-deblurring artifacts. Fig. 3 demonstrates the mask generation method.

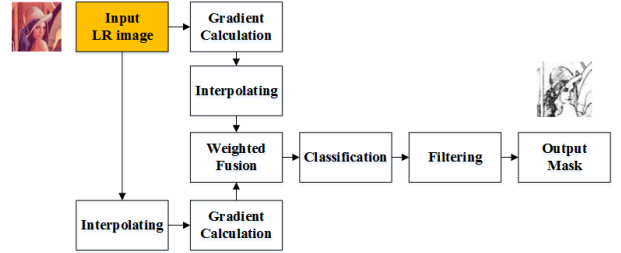


Fig. 3. Multi-resolution mask generation method.

We calculate the gradient map in the interpolated image to determine the high gradient area for deblurring. However, the interpolation process decreases the gradient, which misleads the classification. In order to solve this problem, we use a multi-resolution method which also calculates gradient in LR image, then interpolates the LR gradient map and fuses two maps to enhance the different-scale gradients in edge and texture parts. After that, we use a threshold to classify the gradient map into (0, 1) mask, 0 for high gradient area and 1 for low gradient area. The mask is used as a weight map to fuse the interpolated image and the deblurred image. In the smooth area, we replace the deblurred image with interpolated image to control the over-deblurring. The process is formulated as (6),

$$\text{Final} = \text{Interpo} \times \text{Mask} + \text{Deblurred} \times (1 - \text{Mask}) \quad (6)$$

As shown in Fig. 3, we slightly filter the (0,1) weight map to smooth the weights along the boundary of two areas.

IV. EXPERIMENTS

We have done experiments on various images with different SR factors. Fig. 4 and Fig. 5 show two examples. We compare our algorithm with the nearest neighbour interpolation, bicubic interpolation and Shan et al. [2]. Example-based SR approaches are usually very slow and cannot offer flexible SR factors, so we do not compare with these approaches here. Our experiment platform is the computer with Intel Core i5-2400, 4G RAM, Windows 7 OS 32bit and Matlab 2013b.

Fig. 4 shows that our algorithm performs well on natural images. Fig. 5 shows that our algorithm controls the over-deblurring artifacts when blur kernel estimation is not enough accurate.



Fig. 4. $3\times$ SR example. Our algorithm is compared with nearest neighbour, bicubic and Shan et al. [2]



Fig. 5. Over-deblurring Control example ($2\times$ SR). The σ of Gaussian kernel is 1.5 for both [2] and ours.

TABLE I
RUNNING TIME OF DIFFERENT SR FACTORS

SR times	Running time
$2\times$	2.78s
$3\times$	3.62s
$4\times$	7.96s
$6\times$	15.49s
$8\times$	20.90s

To demonstrate the speed of our algorithm, we super-resolve the example 128×128 image, which is also used in Fig. 4, to different sizes and show the running time in Table I.

V. CONCLUSION

A regularized SR reconstruction algorithm based on two sparsity properties has been proposed in this paper. Using these two sparsity properties, a sharp SR result is achieved and artifacts are controlled. The proposed algorithm can flexibly super-resolve images to any size and runs relatively fast in our experiments. To get rid of matrix computation, our optimization algorithm can be solved in frequency domain, which also guarantees the running speed. In the next step, we are going to implement our algorithm with C++ and use GPU to accelerate it for real-time applications.

ACKNOWLEDGMENT

This work is partially supported by grants from National Key Technology Research and Development Program of the Ministry of Science and Technology of China under contract No.2014BAK10B00, Major National Scientific Instrument and Equipment Development Project of China under contract

No. 2013YQ030967, also with Beida(Binhai) Information Research.

REFERENCES

- [1] S. C. Park, M. K. Park, and M. G. Kang, "Super-resolution image reconstruction: a technical overview," *Signal Processing Magazine, IEEE*, vol. 20, no. 3, pp. 21–36, May 2003.
- [2] Q. Shan, Z. Li, J. Jia, and C.-K. Tang, "Fast image/video upsampling," in *ACM Transactions on Graphics (TOG)*, vol. 27, no. 5. ACM, 2008, p. 153.
- [3] J. Sun, J. Sun, Z. Xu, and H.-Y. Shum, "Image super-resolution using gradient profile prior," in *Computer Vision and Pattern Recognition, 2008. CVPR 2008. IEEE Conference on*, June 2008, pp. 1–8.
- [4] C.-T. Shen, H.-H. Liu, M.-H. Yang, Y.-P. Hung, and S.-C. Pei, "Viewing-distance aware super-resolution for high-definition display," *Image Processing, IEEE Transactions on*, vol. 24, no. 1, pp. 403–418, Jan 2015.
- [5] A. Levin, R. Fergus, F. Durand, and W. T. Freeman, "Image and depth from a conventional camera with a coded aperture," in *ACM Transactions on Graphics (TOG)*, vol. 26, no. 3. ACM, 2007, p. 70.
- [6] E. J. Candes, M. B. Wakin, and S. P. Boyd, "Enhancing sparsity by reweighted l_1 minimization," *Journal of Fourier analysis and applications*, vol. 14, no. 5-6, pp. 877–905, 2008.
- [7] N. Parikh and S. Boyd, "Proximal algorithms," *Foundations and Trends in optimization*, vol. 1, no. 3, pp. 123–231, 2013.
- [8] W. Freeman, T. Jones, and E. Pasztor, "Example-based super-resolution," *Computer Graphics and Applications, IEEE*, vol. 22, no. 2, pp. 56–65, Mar 2002.
- [9] H. Chang, D.-Y. Yeung, and Y. Xiong, "Super-resolution through neighbor embedding," in *Computer Vision and Pattern Recognition, 2004. CVPR 2004. Proceedings of the 2004 IEEE Computer Society Conference on*, vol. 1, June 2004, pp. I–I.
- [10] J. Yang, J. Wright, T. Huang, and Y. Ma, "Image super-resolution via sparse representation," *Image Processing, IEEE Transactions on*, vol. 19, no. 11, pp. 2861–2873, Nov 2010.
- [11] D. Glasner, S. Bagon, and M. Irani, "Super-resolution from a single image," in *Computer Vision, 2009 IEEE 12th International Conference on*, Sept 2009, pp. 349–356.
- [12] X. Li and M. Orchard, "New edge-directed interpolation," *Image Processing, IEEE Transactions on*, vol. 10, no. 10, pp. 1521–1527, Oct 2001.